JOURNAL OF AGRICULTURAL AND FOOD CHEMISTRY

ARTICLE

pubs.acs.org/JAFC

Evaluation of Nonpolar Metabolites in Plant Extracts by ^{13}C NMR Spectroscopy

Martina Palomino-Schätzlein,[†] Pablo V. Escrig,[§] Herminio Boira,[#] Jaime Primo,[⊥] Antonio Pineda-Lucena,[†,⊗] and Nuria Cabedo*[,⊥]

[†]Servicio de Resonancia Magnética Nuclear, Centro de Investigación Príncipe Felipe, Avenida Autopista del Saler 16, 46012 Valencia, Spain

[§]Instituto de Tecnología Química (UPV-CSIC), Universidad Politécnica de Valencia, Avenida de los Naranjos s/n, 46022 Valencia, Spain

[#]Instituto Agroforestal Mediterráneo, Universidad Politécnica de Valencia, Camino de Vera s/n, 46022, Valencia, Spain

[⊥]Centro Ecología Química Agrícola-Instituto Agroforestal Mediterráneo, Universidad Politécnica de Valencia, Avenida de los Naranjos s/n, Edificio 6C, 46022 Valencia, Spain

[⊗]Laboratorio de Bioquímica Estructural, Centro de Investigación Príncipe Felipe, Avenida Autopista del Saler 16, 46012 Valencia, Spain

Supporting Information

ABSTRACT: ^{13}C nuclear magnetic resonance (NMR) spectroscopy was explored as a simple and efficient technique for the quantitative analysis of nonpolar metabolites in plants. The method was first optimized with a mixture of known metabolites and then applied to the nonpolar leaf extracts of plants harvested in the Valencian community (eastern Spain) belonging to three different genera: *Euphorbia* (Euphorbiaceae), *Araujia* (Apocynaceae), and *Morus* (Moraceae). Furthermore, an exhaustive analysis of *Euphorbia characias* leaf and stem extracts from different geographic locations allowed that quantitative ^{13}C NMR spectroscopy is a suitable tool for metabolic profiling purpose.

KEYWORDS: *Euphorbia*, *Morus*, *Araujia*, hydrocarbons, triterpenes, metabolic profiling, quantitative ^{13}C NMR, multivariate analysis

INTRODUCTION

Metabolic profiling has been applied in plant science to an increasing range of biological questions: agrochemical development, plant metabolite engineering, plant secondary metabolism, plant growth and response to stress, functional genomics, and plant breeding and nutrition, with applications in food chemistry, agriculture, medicine, and ecology.[1,2] The plant metabolome is extensive and complex. Estimates of metabolome size for an individual plant vary within the 5000−10000 range, with a total of up to 200,000 different structures occurring in the plant kingdom.[3]

Nonpolar extracts of higher plants consist of complex mixtures of long-chain aliphatic and cyclic components (≥C20), including hydrocarbons, primary and secondary alcohols, aldehydes, ketones, esters, fatty acids, and triterpenoids. These nonpolar constituents are ubiquitous in cuticular waxes[4] and in the latex of some angiosperm families, especially in the Euphorbiaceae.[5] Cuticular waxes have very different physiological functions (control of water loss and leaf temperature, photoprotection, and frost hardness) and play an ecological role in the interaction with insects and pathogens.[4] Latex's role in the plant is not well-known, but it has been suggested to be defensive against herbivores and pathogens.[6] In addition, alkanes and triterpenoids have been regarded as potential chemotaxonomic markers as they could differentiate between groups of plant species that share both ecological and genetic factors.[7]

In this context, nuclear magnetic resonance (NMR) spectroscopy is a very suitable method because it allows the simultaneous detection of diverse groups of primary and secondary metabolites. In the NMR spectrum, signal intensities are proportional to their concentrations, thus enabling the direct comparison of the concentrations of all compounds, without the need of calibration curves for each individual compound. In addition, NMR spectroscopy is a very useful nondestructive technique for the structure elucidation of metabolites. In particular, two-dimensional experiments allow the identification of signals without requiring a further fractionation of the extract or chemical treatment. Several methods have been described for the NMR-based analysis of polar plant metabolites in the classification and characterization areas of medical plants, monitoring response to stress, wounding or infection of plants, or discriminating wild and transgenic.[8] However, the study of the metabolite profile of nonpolar extracts by NMR has been applied only in limited cases.[9] One reason for the limited application of NMR to the nonpolar metabolite profile is the high degree of overlapping of nonpolar metabolite signals in the ^{1}H NMR spectrum, making the identification of each compound difficult. ^{13}C NMR spectroscopy dramatically diminishes the signal overlap problem found in ^{1}H spectra because the chemical shift range is >20 times higher. In addition, all scalar couplings are removed by ^{1}H decoupling, thus simplifying the spectrum to a single line for each chemically nonequivalent carbon. The main drawback of ^{13}C spectroscopy is its poor sensitivity due

Received: August 1, 2011
Revised: September 26, 2011
Accepted: September 28, 2011
Published: September 28, 2011

dx.doi.org/10.1021/jf2030902 | J. Agric. Food Chem. 2011, 59, 11407–11416

to the low natural abundance (~1.1%) and the low gyromagnetic ratio (~25% of ^{1}H) of ^{13}C nuclei. Yet NMR signal-to-noise ratios (S/N) can be significantly improved by cooling the NMR radio frequency detector and preamplifier.[10] This improved sensitivity for ^{13}C nuclei is such that cryogenic probes allow good S/N with reasonable acquisition times. Therefore, the use of cryogenic probes for ^{13}C NMR has provided an additional tool for metabolomics, as proven for the biofluids analysis.[11] To the best of our knowledge, cryogenic probes for ^{13}C NMR have not yet been exploited for the metabolic profiling of plants, although conventional ^{13}C NMR spectroscopy has been reported for the quantification of plant components.[12−14]

This work reports the application of quantitative ^{13}C NMR spectroscopy using a cryoprobe as a simple and efficient technique for the quantitative analysis of nonpolar metabolites in plants, which are usually analyzed by liquid or gas chromatography coupled to mass spectrometry (LC-MS and GC-MS). The method, after optimization with a mixture of known metabolites, was applied to leaf extracts of higher plants harvested in the Valencian community (eastern Spain) belonging to three different genera: *Euphorbia*, *Araujia*, and *Morus*. These angiosperms were chosen for their availabilities and high contents in nonpolar metabolites. Furthermore, we carried out an exhaustive analysis of *E. characias* leaf and stem extracts as a model plant to validate quantitative ^{13}C NMR spectroscopy for metabolite profile purpose.

MATERIALS AND METHODS

Reagents. Reference compounds (nonacosane, 1-hexadecanol, α-amyrin, α-amyrin acetate, caryophyllene, cycloartenol, ergosterol, lanosterol, lupeol, lupenone, phytol, stigmasterol, β-sitosterol, squalene, α-tocopherol, palmitic acid, linoleic acid, oleic acid), chromium(III) triacetylacetonate ($Cr(acac)_3$), and chloroform-*d* were purchased from Sigma-Aldrich Co. (St Quentin Fallavier, France). Hexanes, ethyl acetate, dichloromethane, THF, and methanol were purchased from Scharlab S.L. (Barcelona, Spain). All reagents and solvents were of analytical grade.

Plant Materials and Extraction. Plant specimens were collected from the Valencian community (eastern Spain). *Morus alba* (MA, white mulberry) and *Araujia sericifera* (AS, bladder flower) were collected in the summer season (September 2009 and 2010, respectively) in Castellon. Wild populations of the model plant *Euphorbia characias* (EC, Mediterranean spurge) were collected in July 2009 (for metabolic profiling) and September 2009 (for comparative analysis with MA and AS). EC plants were harvested from three different areas: the Mariola Mountains (Alicante) and the Alt Maestrat region (Castellon), both at 1000 m above sea level, as well as the Espadan Mountains (Castellon) at 400 m altitude. The geographical distance between the two more distant locations is about 200 km (the Mariola Mountains and the Alt Maestrat or the Mariola and the Espadan Mountains) and the minimal distance between the locations is about 80 km (the Alt Maestrat and the Espadan Mountains). From each population, samples were carefully collected in the morning from mature plants, excluding any tissues with necrotic or chlorotic regions. Three to five independent samples of leaves and stems (for EC) from the three regions were analyzed.

Fresh leaves of the plants (also stems for EC) were separated, snap-frozen in liquid nitrogen, ground using a mortar and pestle, and freeze-dried.[15] The dry powdered aerial parts of the plants (0.4−0.5 g) were placed in a 250 mL Erlenmeyer flask and extracted three times by maceration with CH_2Cl_2 followed by EtOAc (25 mL of each solvent per 0.5 g of the dry plant) and stirring at room temperature for 20 min. The organic extracts were filtered, combined, and reduced to approximately 1 mL by rotatory evaporation under reduced pressure and then filtered through a 0.45 μm syringe filter. The filtrate was taken to dryness under a nitrogen stream to give the residues of the corresponding extracts, which were stored at −20 °C until their analysis.

NMR Spectroscopy. Immediately before the NMR acquisition the extract was defrosted at room temperature, and NMR samples were prepared by dissolving 30−40 mg of the crude extract in 500 μL of $CDCl_3$ and 1 μL of DMF as internal standard; furthermore, 60 mM $Cr(acac)_3$ as relaxation agent was added in the case of quantitative ^{13}C NMR spectra. NMR spectra were recorded at 25 °C on a Bruker AVII-600 using a 5 mm TCI cryoprobe (quantitative ^{13}C spectra) and a Bruker AVIII-500 using a 5 mm TBI probe (all the other experiments) and processed using Topspin 2.16 software (Bruker GmbH, Karlsruhe, Germany). Quantitative ^{13}C NMR spectra were acquired using the inverse gated decoupling pulse sequence[16] where the nuclear Overhauser effect is avoided. A total of 6000−8000 transients were collected depending on the sample concentration with 32K data points (acquisition time = 0.5 s) over a spectral width of 200 ppm. A 5 s relaxation delay was incorporated between each scan. Spectra were processed using an exponential weighting function (lb = 1) and zero filling to 64K. Nonquantitative ^{13}C NMR spectra were obtained using a standard ^{1}H-decoupled sequence. Five hundred and twelve transients were collected with 32K data points over a spectral width of 200 ppm. A 2 s relaxation delay was incorporated between each scan. Spectra were processed using an exponential weighting function (lb = 1) and zero filling to 64K.

The NMR data of the identified metabolites are well documented, and ^{13}C NMR spectral assignments were made by comparison of the observed chemical shift values with the reported values.[17−20] Not only the 1D chemical shifts but also the corresponding ^{13}C and ^{1}H correlations from 2D experiments were compared with the literature values to do unequivocal assignments. For compounds with an important structural complexity, reference samples with commercial compounds were prepared and 2D NMR spectra were acquired. The superimposition of the 2D spectra of the standards and the extracts allowed the unambiguous confirmation of each compound present in the complex extract. Double-quantum-filtered correlation spectroscopy (DQF-COSY), total correlation spectroscopy (TOCSY), heteronuclear multiple-bond correlation (HMBC), and multiplicity edited heteronuclear single-quantum correlation (HSQC) were all collected using standard experimental sets for representative extract samples and all reference compounds. For each of these experiments, 256−512 points in the indirect dimension increments were used and 32−96 transients were collected. The relaxation delays were set to 1.5 s.

Data Reduction. Two different methods are commonly used for the conversion of the spectra in data matrices for multivariate analysis (MVA):[21] rectangular bucketing, where the spectrum is divided into equal regions (normally 0.01−0.04 ppm) and integrated, or variable-sized bucketing, where exact regions corresponding to isolated or superposed signals for each integral are defined, allowing the exclusion of all spectral regions without signals. Both methods were applied between 5 and 200 ppm to our data using Amix (v. 3.9.7, Bruker GmbH), and both data matrices gave similar results after MVA. However, variable-sized bucketing allows working with much smaller data matrices, and the interpretation of the loading plots from MVA is much easier. For this reason this seems to be the best option for ^{13}C spectra analysis and the method chosen to present our results in metabolic profiling.

Normalization and Scaling. Buckets were normalized with Amix to the sum of total spectral intensity to minimize differences in sample concentration. Solvent signals as well as the signals of the internal standard were excluded from the bucketing and the normalization area. Furthermore, scaling is recommended for an easier interpretation of the data and takes into account the small signals. In the case of spectroscopic data, where all variables are expressed in the same unities but we have a high metabolite concentration range, Pareto scaling is often the best choice.[22] In this method, each value is divided by the square root of the standard deviation of each variable, and it represents an optimal intermediate between no scaling and unit variance scaling (where each

value is divided by the standard deviation of each variable). Additionally, mean centering is applied to the scaled data to improve the interpretability of the model. Both scaling and centering were done with Simca-P+ 12.0 (Umetrics, Umeå, Sweden).

Multivariate Data Analysis. After normalization and scaling, data were subjected to MVA with Simca-P+ 12.0. Principal component analysis (PCA), an unsupervised pattern recognition method,[23] was used as an initial overview of the information in the data table. PCA score plots show clustering trends between samples, how metabolite concentrations are related, and if there are any strong outliers. Furthermore, distance to model (DmodX) plots were examined for moderate outliers.

To fine-tune the analysis and build a discrimination model, a supervised classification method was used. Recently, orthogonal projection on latent structure-discriminant analysis (OPLS-DA)[24] has been introduced as optimal discriminant analysis for metabolomic plant data. The advantage of OPLS-DA versus the PLS-DA,[25] which has been widely applied in metabolomics, is that OPLS-DA separates predictive variation (between classes) from nonpredictive (within classes) variation, whereas in PLS-DA two or more components may be required. Thus, clear separations in the score plots are obtained and discriminant metabolites can be easily identified from the corresponding loading and S-plots.[26] OPLS-DA analysis was performed by dividing the samples in different classes according to the origin of the plant (the Mariola Mountains, the Alt Maestrat, and the Espadan Mountains) or the part of the plant (stems and leaves).

Model Validation. If more than 10 samples were available for each class, the OPLS-DA model was validated by prediction. To this end, samples were divided in two sets, and one set was used for the OPLS-DA model definition. The class membership of the remaining data was then predicted using the OPLS-DA model. Fisher's probability of <0.01 is considered to be a good prediction. This is a very severe and robust test, widely employed for model validation in metabolomics.[27] For fewer samples, cross-validation was performed with a permutation test 20 times.[28] Prediction coefficients Q^2 generated from the permutation test were compared to the Q^2 value of the real model. If the intercept Q^2 value from the permutation test was smaller than Q^2 of the real model, the model was regarded as predictable.

NMR Integration. Each region of the ^{13}C NMR spectrum defined in the Supporting Information (Tables S1−S3) was integrated in MestReNova (v 6.2.0−7238, 2010 Mestrelab Research S.L.) with the multiple integration option. Concentrations (mmol/g of extract) were determined in relation to the internal standard (DMF) concentration. In the case of the metabolic study of EC samples, signals were normalized to the sum of total spectral intensity for a better comparison. A mean integral of the different spectral regions corresponding to the same molecule or group of molecules was calculated, and the values of the independent samples done for each condition (region and part of the plant) were averaged. Significant differences between groups were calculated with a two-way analysis of variance (ANOVA) and the Tukey range test. Statistical calculations were calculated with SPSS (v 14.0, SPSS Inc., 1989−2005), and graphics were represented with Excel.

RESULTS AND DISCUSSION

Optimization with a Known Mixture of Nonpolar Metabolites. Quantitative ^{13}C spectroscopy is not as straightforward as quantitative ^{1}H NMR spectroscopy.[29] In conventional ^{13}C NMR, the nuclear Overhauser effect (NOE) is applied to enhance signal intensity, but the achieved increment is not the same for all resonances; thus, signal intensity is not proportional to molar concentration. For quantitative determinations, a special pulse program with inverse gated decoupling is used, in which the NOE is suppressed.[16] On the other hand, long delays have to be incorporated between experiments to ensure the relaxation of all ^{13}C resonances, which results in long acquisition times. To prevent this, a relaxation reagent to shorten the T_1 (relaxation time) value is added to the samples. In our case, the shiftless paramagnetic agent chromium(III) triacetylacetonate ($Cr(acac)_3$) was chosen, which has been successfully applied in several studies.[30] The addition of $Cr(acac)_3$ must be done cautiously, as excess will increase relaxation rates to the extent that resonances will broaden (fast T_2 relaxation) and will be difficult to detect. To optimize the $Cr(acac)_3$ concentration, an inversion/recovery NMR experiment was performed on a sample containing five selected secondary metabolites (model mixture A, nonacosane, lupeol, stigmasterol, phytol, and tocopherol) at known concentrations. The T_1 value was calculated for different $Cr(acac)_3$ concentrations (Table 1). The best result was obtained for 60 mM $Cr(acac)_3$ as T_1 was considerably reduced (0.7s) and the spectral resolution still fell in a good range (line width at half height < 1.5 Hz). Furthermore, no important chemical shift changes were observed. The integration of the quantitative ^{13}C spectrum of the known model mixture A with 60 mM $Cr(acac)_3$ resulted in concentration values that were in good agreement with the theoretical values (Table 2). To better simulate the

Table 1. T_1 Values Obtained for Different Concentrations of $Cr(acac)_3$ of Model Mixture A[a]

conc of $Cr(acac)_3$ (mM)	T_1 (s)	conc of $Cr(acac)_3$ (mM)	T_1 (s)
0	9.0	60	0.7
35	1.5	85	0.5

[a] T_1 values have been calculated using the equation $T_1 = t_{null}/\ln 2$ and are approximated.

Table 2. Percentage of Each Compound Obtained from the Integration of the Quantitative ^{13}C Spectrum of Model Mixture A with 60 mM $Cr(acac)_3$[a]

		percentage (%)	
compd	wt (mg)	of wt	calcd by NMR
tocopherol	5.9	4.8	4.6
phytol	32.6	38.4	35.0
lupeol	4.1	3.4	3.3
stigmasterol	27.4	23.2	24.0
nonacosane	35.5	30.3	32.5

[a] Compounds were dissolved in 500 μL of $CDCl_3$.

Table 3. Percentage of Each Compound Obtained from the Integration of the Quantitative ^{13}C Spectrum of Model Mixture B with 60 mM $Cr(acac)_3$[a]

		percentage (%)	
compd	wt (mg)	of wt	calcd by NMR
1-hexadecanol	7.0	52.0	50.8
ergosterol	1.1	8.4	9.8
phytol	0.3	1.8	1.7
squalene	3.1	23.0	22.7
stigmasterol	1.2	8.6	8.9
tocopherol	0.8	6.0	6.1

[a] Compounds were dissolved in 500 μL of $CDCl_3$.

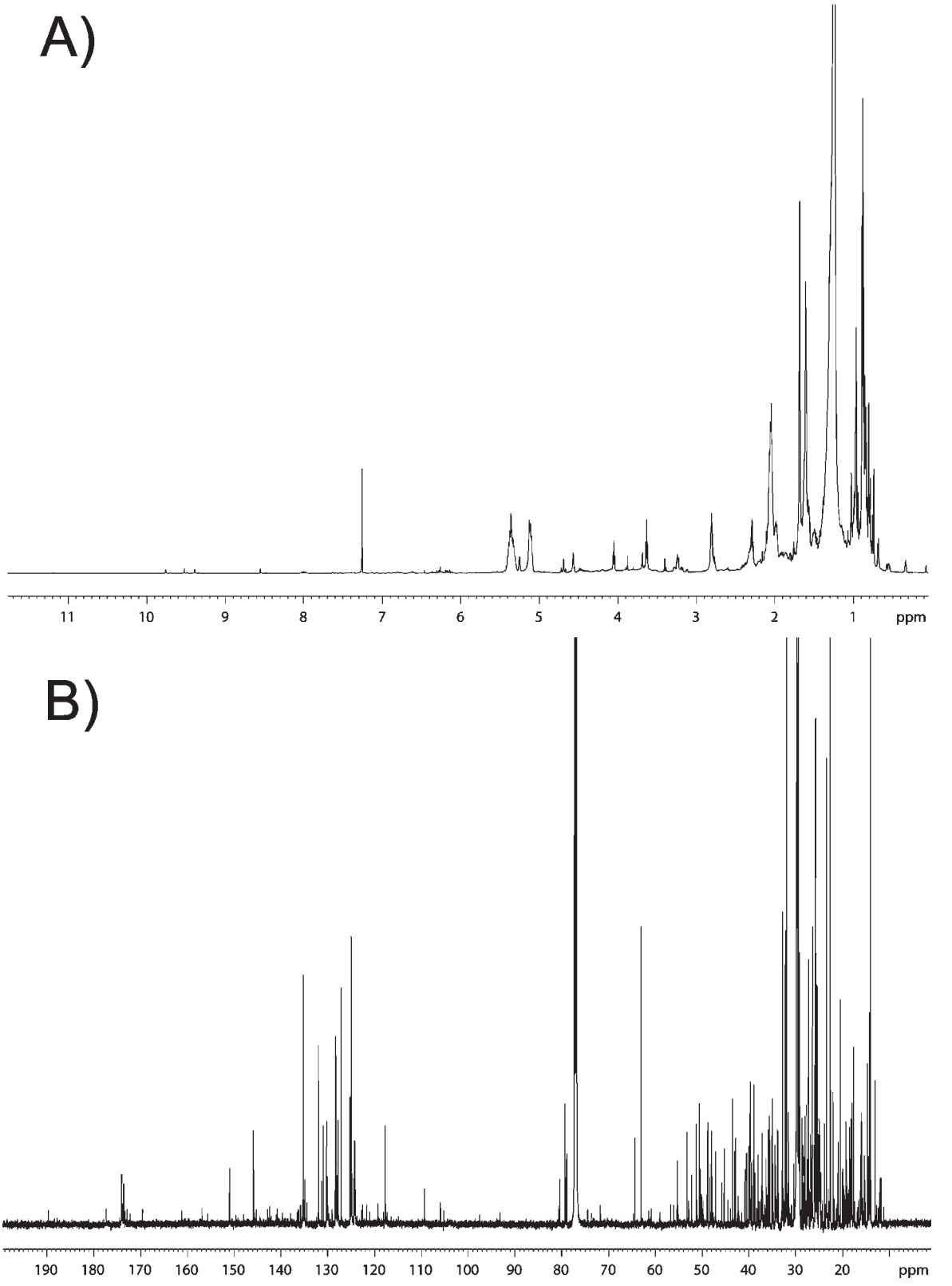

Figure 1. NMR spectra of an EC leaf extract (40 mg) dissolved in 500 μL of $CDCl_3$: (A) ^1H spectrum; (B) ^{13}C spectrum (60 mM $Cr(acac)_3$ was added).

real sample conditions and obtain a better estimation of the integration error, a second known mixture with lower amounts of each selected secondary metabolite (model mixture B, 1-hexacosanol, ergosterol, phytol, lupeol, stigmasterol, and nonacosane) was prepared. Once again, good results were obtained (Table 3).

Analysis of the Crude Plant Extracts. After optimization of the quantitative ^{13}C NMR experiment for mixtures (A and B) of

Table 4. Concentration of Metabolites in Leaf Extracts of AS, EC, and MA Determined by Quantitative ^{13}C NMR Spectroscopy

	concn (mmol/g of extract, mean ± SEM)[a]		
	AS	EC	MA
$CH_3CH_2CH_2CH_2-$	0.602 ± 0.038	1.281 ± 0.504	1.052 ± 0.010
cis-polyisoprene	1.634 ± 0.466	0.623 ± 0.322	0.534 ± 0.007
free acids, −COOH	0.306 ± 0.063		0.514 ± 0.058
esters, $-CH_2OCO-$	0.049 ± 0.016	0.109 ± 0.048	0.032 ± 0.000
free alcohols, $-CH_2OH$		0.235 ± 0.098	
TAG	0.016 ± 0.013		
linolenic ester/acid	0.039 ± 0.006	0.087 ± 0.049	0.514 ± 0.058
squalene	0.098 ± 0.022		0.275 ± 0.115
triterpen-3-ols, $-CH_2OH$	0.350 ± 0.041	0.774 ± 0.295	
triterpene esters, $-CH_2OR$	0.361 ± 0.007	0.226 ± 0.106	0.053 ± 0.007
germanicol derivatives	0.177 ± 0.009		
triterpen-3-propionate	0.002 ± <0.001		
triterpen-3-cinnamate	0.132 ± 0.004		
triterpen-3-(2-methyl-2-butenoate)	0.103 ± 0.006		
lupeol	0.234 ± 0.006	0.123 ± 0.043	
lupeol-3-acetate	0.112 ± 0.036	0.002 ± 0.001	0.053 ± 0.007
lupen-3-one		0.002 ± 0.001	
lanosterol derivatives		0.033 ± 0.014	0.061 ± 0.016
butyrospermol		0.194 ± 0.090	
cycloartenol derivatives		0.209 ± 0.065	
24-mehtylenecycloartenol		0.071 ± 0.014	
cycloartenol		0.136 ± 0.065	
25-hydroperoxycycloart-23-en-3β-ol		0.022 ± 0.007	
α-amyrin		0.030 ± 0.012	0.082 ± 0.000
α-amyrin acetate			0.055 ± 0.000
chlorophyll			0.064 ± 0.019
β-sitosterol	0.049 ± 0.001	0.025 ± 0.009	0.041 ± 0.005

[a] Each value represents the average and the standard error of the spectra of three independent experiments.

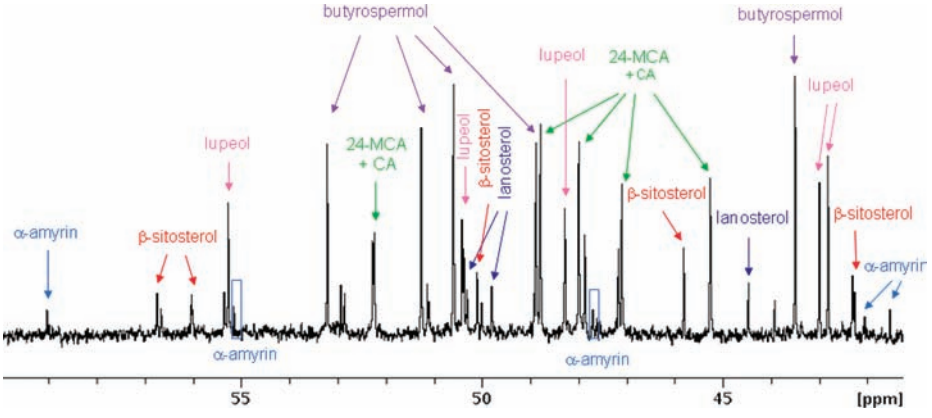

Figure 2. ^{13}C NMR assignment of an EC leaf extract (40 mg) dissolved in 500 μL of $CDCl_3$.

nonpolar plant metabolites, the real extracts of the three plants, *E. characias* (EC), *M. alba* (MA), and *A. sericifera* (AS) were analyzed. A simple sample preparation procedure was followed. The T_1 value of ^{13}C was determined for an EC leaf extract sample in the absence and presence of 60 mM relaxation agent for the purpose of seeing the effect of $Cr(acac)_3$ on the real samples. The T_1 values for the quaternary carbons were 36 s without $Cr(acac)_3$ and 1 s with $Cr(acac)_3$ (Figures S-1 and S-2, Supporting Information). This means that a relaxation delay ($D^1 \sim 5T_1$) of 5 s could be used for samples with 60 mM $Cr(acac)_3$, with results in a reasonable acquisition time. ^{1}H spectra and quantitative ^{13}C spectra were acquired for all samples. As expected, the degree of overlap was very high in the ^{1}H NMR spectrum, whereas the ^{13}C NMR spectrum displayed much greater dispersion, as seen for the EC leaf extract sample (Figure 1).

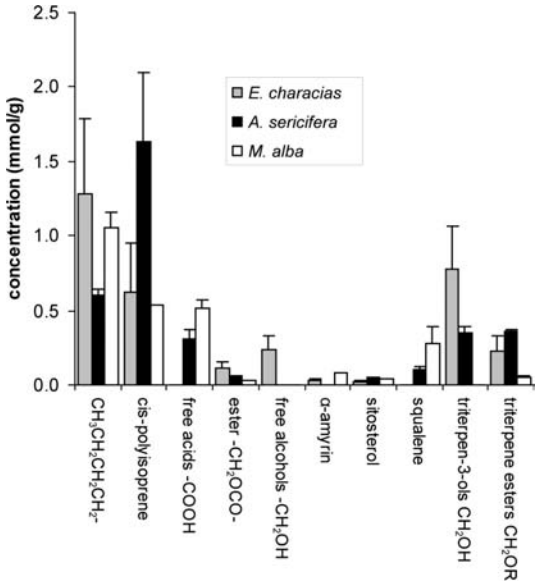

Figure 3. Composition of the main metabolites in the nonpolar EC, AS, and MA leaf extracts. Concentration is given in mmol/g of extract.

The metabolites were identified and quantified for all three plants in the leaf extracts (Table 4). A section of the assigned ^{13}C of EC extract is represented in Figure 2. In this part of the spectrum (40−60 ppm), few signal overlaps take place and most signals are unambiguously identified, which was not possible for the ^{1}H spectrum. The exact integration regions used for each compound or group of compounds can be found in the Supporting Information. The characteristic signals of alkanes, fatty acids, esters, and alcohols were clearly identified, even if the NMR spectra did not allow the determination of the exact chain length of the molecules (Table 4). Furthermore, a characteristic region for triterpen-3-ols and triterpene esters at 78.4−79.2 and 80.4−81.2 ppm, respectively, was assigned, thus allowing the determination of the total quantity of this family of compounds in extracts. The main advantage of NMR is that, unlike GC-MS and HPLC-MS, all kinds of molecules are detected irrespective of their molecular weight and functional groups.

Figure 3 depicts a comparison of the main metabolite types found in the leaf extracts of the studied plants. Some significant observations included the high *cis*-polyisoprene content found in the AS extracts, whereas MA extracts stood out for their high free acids content (mainly linolenic acid). In the three plants of our study, tetracyclic and pentacyclic triterpenes represented the most important group of secondary metabolites. These constituents have an agricultural interest because of their antifeedant, chemosterilant, and insect growth inhibitor properties, which have been already reported for several tetracyclic triterpenes isolated from the latex of *Euphorbia* species.[31] In our study, EC leaf extracts were emphasized for the highest triterpene content, whereas MA extracts revealed the lowest triterpene profiles, particularly triterpen-3-ols. A small number of metabolites were found exclusively in some of these three plants. For instance, cycloartenol derivatives were found only in the EC leaf extracts, whereas germanicol derivatives were characteristic of the AS extracts. Cinnamoyl and 2-methyl-2-butenoyl acids were esterified with triterpen-3-ols only in the AS leaf extracts. In contrast, lupeol derivatives were detected at high levels in the three extracts. The only sterol found, β-sitosterol, was present in all leaf extracts in similar amounts (Table 4).

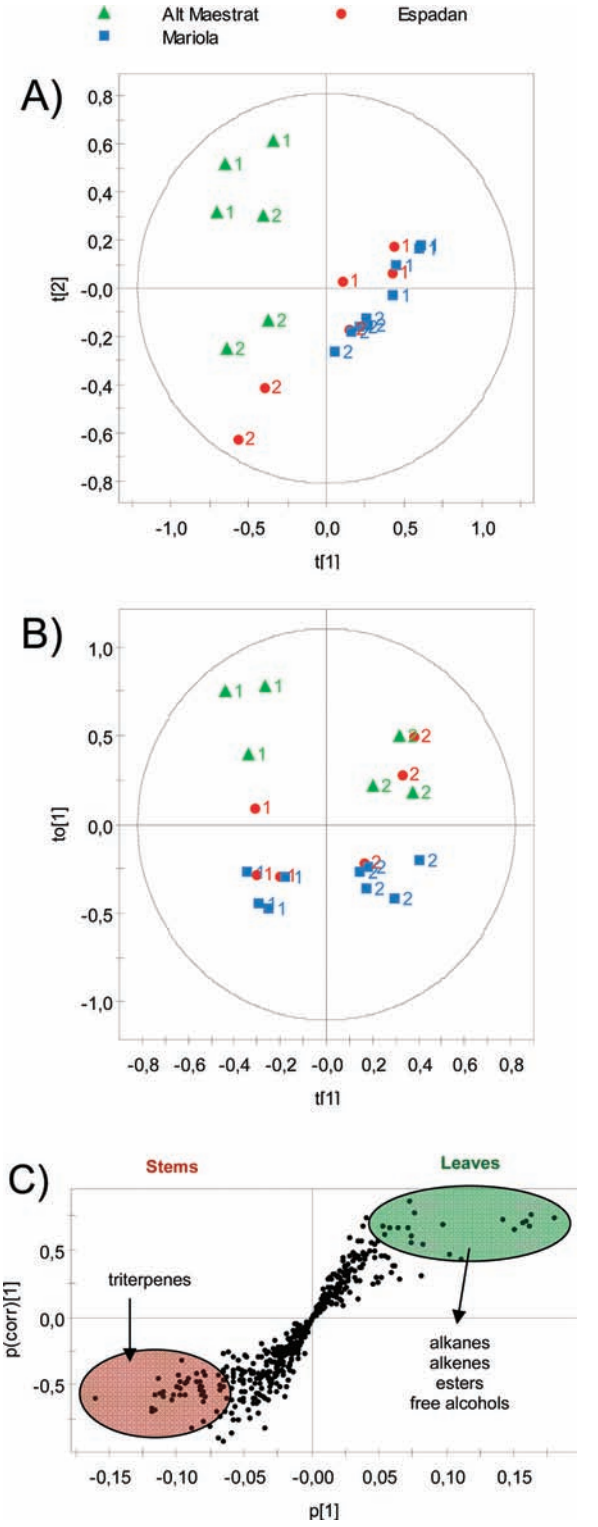

Figure 4. Multivariate analysis of ^{13}C spectra of nonpolar EC extracts: (A) Two components of unsupervised PCA model, PC1 and PC2, explain 38 and 17% of the variation, respectively. (B) 1 + 1 component supervised OPLS-DA model. Samples from stems and leaves were defined as two different classes. $R^2Y_{cum} = 0.92$, $R^2X_{cum} = 0.53$, $Q^2_{cum} = 0.88$. Fishers probability from prediction test = 0.004. (C) Visualization of OPLS-DA loadings in the form of an S-plot: the magnitude of each loading (p) is represented in front of the reliability of each loading (p_{corr}). Stem and leaf samples are represented with the numbers 1 and 2, respectively.

Most of these metabolites were already found in the latex and epicuticular wax compositions of EC and other *Euphorbia* species, which have been extensively studied for their composition in bioactive compounds.[31,32] Leaves of MA have been reported to contain many secondary metabolites that are responsible for health benefits. Among them, β-sitosterol and several triterpenes have exhibited inhibitory effects on triglyceride accumulation.[33] Less attention has been focused on the nonpolar metabolites of the invasive weed AS. In fact, triterpenic compounds have not been previously identified in leaves, and only three triterpenes were isolated from the fruits of AS, including the germanicol acetate with antihistamic activity.[34] The presence of diverse triterpenes in the leaf extract of the plant could lead to interesting agricultural and pharmacological applications.

The metabolites presented in our studied plants (EC, AS, and MA) were also isolated and/or produced by other agriculturally important plants. Thus, cycloartenol, 24-methylenecycloartenol, and β-sistosterol together with other triterpene alcohols and sterol ferulic acid esters were found in one of the major bioactive components in rice brain oil, γ-oryzanol, a byproduct of the rice milling process with blood lipid lowering activity.[35] Several pentacyclic triterpenes, including lupane (lupeol and lupeol-3-acetate) and oleanane (germanicol) carbon skeletons with insect antifeedant properties and phytotoxic effects, were isolated from *Pericallis lanata* and *Salvia broussonetti*.[31] Commercial cork of *Quercus suber* and industrial cork byproducts can also be considered as abundant sources of triterpenic compounds.[36] Olive (*Olea europea*) fruit and leaf were reported to contain *n*-alkanes, fatty acids, alkyl esters, and a wide variety of sterols and triterpenoids in their epidermis.[37]

Metabolic Profiling of the Model Plant (EC). To validate the method for metabolic profiling purposes, EC was chosen as a model plant and was exhaustively studied. Leaf and stem samples from three different regions in the area of study (the Mariola Mountains, the Espadan Mountains, and the Alt Maestrat) were analyzed to evaluate the influence of the climatic and environmental factors on the metabolite profile. The Mariola and Espadan Mountains are Mediterranean forest regions located in the lower mesomediterranean bioclimatic belt, whereas the Alt Maestrat is located in the higher mesomediterranean bioclimatic belt, which is characterized by scrub vegetation.[38] Quantitative ^{13}C spectra of samples from leaf and stem extracts from the three regions were obtained.

MVA based on projection methods can prove to be most useful in metabolomics, as it converts the complicated matrices obtained from multiple data points into fewer, information-rich parameters. Metabolic fingerprinting performed in this way can be used to classify samples on the basis of their comprehensive metabolite profile. The first approach opted for our data was to apply a MVA in the form of a PCA to get a simple overview of the information of the data table. For this purpose, spectra were processed and analyzed as described under Materials and Methods. The score plot of the first two principal components (Figure 4A) showed interesting clustering trends. All samples corresponding to stem extracts were placed at the upper part of the plot, whereas most samples from leaves were situated at the lower part. Furthermore, a clear separation of samples from the Alt Maestrat with respect to samples from the Mariola and the Espadan Mountains took place. Even some differences between samples from the Mariola and Espadan Mountains could be detected.

To get a more defined class separation and identify the metabolites that were characteristic for each group, OPLS-DA was

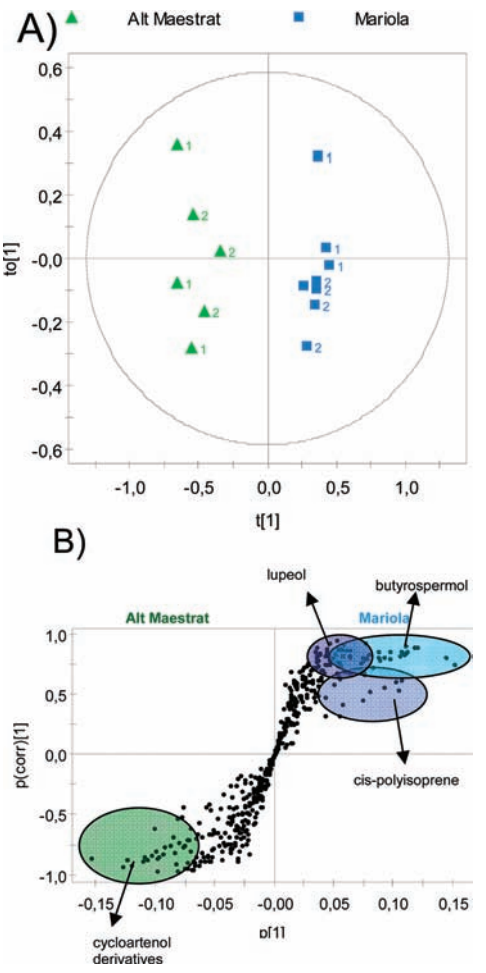

Figure 5. Multivariate analysis of ^{13}C spectra of nonpolar EC extracts from the Alt Maestrat and Mariola regions. (A) 1 + 1 component supervised OPLS-DA model. Samples from the Alt Maestrat and Mariola regions were defined as two different classes. R^2Y_{cum} = 0.97, R^2X_{cum} = 0.52, Q^2_{cum} = 0.92. Permutation test: Q^2 = −0.33. (B) Visualization of OPLS-DA loadings in the form of an S-plot: the magnitude of each loading (p) is represented in front of the reliability of each loading (p_{corr}). Stem and leaf samples are represented with numbers 1 and 2, respectively.

performed. Figure 4B shows the OPLS-DA score plot in which samples from stems and leaves were defined as two different classes. As can be seen, a sharp, vertical separation between the two kinds of samples was obtained (R^2Y_{cum} = 0.92 and Q^2_{cum} = 0.88). When only half of the samples were used for model building, a very similar OPLS-DA model was obtained. Applying this model to the second subset of samples allowed a correct prediction, in all cases, with a high confidence (Fisher's probability = 0.004).

For the identification of the most relevant metabolites, the corresponding loading in form of an S-plot (Figure 4C) was used. Stem samples could be correlated with high amounts of butyrospermol, cycloartenol derivatives, and triterpenes in general, whereas leaf samples stood out with high amounts of alkanes, esters, and free alcohols. A possible reason for this difference may be the higher abundance of triterpene-rich latex in the stems of *Euphorbia* species.[5]

It was difficult to analyze the differences between regions with only one OPLS-DA model, because only a slight separation between the Mariola and Espadan samples was observed, whereas the

Table 5. Relative Amounts of Metabolites in *E. characias* Extracts

		mean ± SEM[a]										
		Mariola Mountains		Alt Maestrat		Espadan Mountains		leaves/stems		regions		
	compd	leaves	stems	leaves	stems	leaves	stems	p value[b]	abun	p value[b]	abun	LSD[c] <5%
(1)	**1**	0.176 ± 0.030	0.073 ± 0.006	0.124 ± 0.041	0.063 ± 0.023	0.158 ± 0.055	0.069 ± 0.017	0.003	L > S	0.731		0.061
	2	0.077 ± 0.007	0.149 ± 0.004	0.083 ± 0.020	0.132 ± 0.045	0.065 ± 0.008	0.134 ± 0.001	0.006	L < S	0.938		0.051
	3	0.009 ± 0.003	0.054 ± 0.009	0.021 ± 0.003	0.037 ± 0.010	0.013 ± 0.011	0.063 ± 0.025	0.013	L < S	0.493		0.032
	4	1.671 ± 0.055	2.782 ± 0.096	1.835 ± 0.578	2.873 ± 0.249	1.939 ± 0.129	3.092 ± 0.440	0.001	L < S	0.883		0.845
(2)	**5**	1.116 ± 0.092	1.779 ± 0.557	0.397 ± 0.254	0.450 ± 0.362	0.518 ± 0.378	1.168 ± 0.456	0.058		0.020	AM < M, E	0.885
	6	0.064 ± 0.004	0.086 ± 0.018	0.009 ± 0.005	0.011 ± 0.006	0.066 ± 0.011	0.049 ± 0.002	0.454		<0.001	AM < M, E	0.028
	7	0.297 ± 0.026	0.324 ± 0.046	0.080 ± 0.006	0.127 ± 0.019	0.239 ± 0.038	0.295 ± 0.044	0.209		<0.001	AM < M, E	0.093
	8	0.056 ± 0.008	0.042 ± 0.008	0.093 ± 0.011	0.121 ± 0.022	0.063 ± 0.029	0.045 ± 0.010	0.918		0.002	AM > M, E	0.034
(3)	**9**	2.746 ± 0.108	2.242 ± 0.111	2.553 ± 0.276	2.001 ± 0.165	3.188 ± 0.121	2.494 ± 0.115	0.006	L > S	0.043	AM < M < E	0.744
	10	0.475 ± 0.026	0.026 ± 0.009	1.172 ± 0.165	0.200 ± 0.057	0.388 ± 0.040	0.030 ± 0.015	<0.001	L > S	<0.001	AM > M > E	0.175
	11	0.227 ± 0.023	0.078 ± 0.009	0.087 ± 0.044	0.033 ± 0.018	0.170 ± 0.020	0.088 ± 0.017	0.002	L > S	0.018	AM < E < M	0.059
	12	0.382 ± 0.016	0.727 ± 0.114	0.062 ± 0.008	0.104 ± 0.047	0.184 ± 0.136	0.533 ± 0.155	0.002	L < S	<0.001	AM < E < M	0.217
	13	0.436 ± 0.029	0.567 ± 0.040	0.789 ± 0.040	1.585 ± 0.126	0.571 ± 0.043	0.648 ± 0.083	<0.001	L < S	<0.001	AM > E > M	0.100
	14	0.095 ± 0.006	0.133 ± 0.013	0.242 ± 0.044	0.483 ± 0.101	0.117 ± 0.026	0.190 ± 0.025	0.016	L < S	0.001	AM > E > M	0.115
(4)	**15**	0.250 ± 0.175	0.023 ± 0.010	0.451 ± 0.381	0.080 ± 0.053	0.025 ± 0.011	0.022 ± 0.011	0.289		0.291		0.381
	16	0.264 ± 0.030	0.325 ± 0.058	0.327 ± 0.105	0.545 ± 0.245	0.143 ± 0.080	0.271 ± 0.059	0.188		0.179		0.281
	17	0.076 ± 0.027	0.268 ± 0.107	0.203 ± 0.114	0.411 ± 0.138	0.320 ± 0.044	0.390 ± 0.045	0.094		0.496		0.312

[a] Integral values are normalized to the sum of total spectral intensity. [b] p values were obtained from a two-way analysis of variance. [c] LSD values were obtained from the application of the Tukey test. Compounds: **1**, esters (CH_2COO); **2**, lanosterol; **3**, lupen-3-one; **4**, triterpenes; **5**, *cis*-polyisoprene; **6**, α-amyrin; **7**, lupeol; **8**, β-sitosterol; **9**, alkanes ($CH_3CH_2CH_2CH_2$); **10**, free alcohols (CH_2OH); **11**, esters (CH_2CH_2OCO); **12**, butyrospermol; **13**, cycloartenol derivatives; **14**, 24-methylenecycloartenol; **15**, linolenic ester; **16**, cycloartenol; **17**, 25-hydroperoxycycloart-23-en-3β-ol. Abun, abundance. L, S, AM, M, E, leaves, stems, Alt Maestrat, Mariola Mountains, and Espadan Mountains, respectively.

separation with the Alt Maestrat samples was noteworthy. The model would be dominated by the differences between the Alt Maestrat and the other two regions, whereas variation between the Mariola and Espadan Mountains would be much worse represented. For this reason, we built three different OPLS-DA models: one for samples from the Alt Maestrat and Mariola Mountains (Figure 5A), one for samples from the Alt Maestrat and Espadan Mountains (Figure S-3, Supporting Information), and one for samples from the Mariola and Espadan Mountains (Figure S-4, Supporting Information). In all cases a good separation was obtained with high Q^2_{cum} values. The models were validated with the permutation test, obtaining low Q^2 intercept values (−0.33, −0.38, and −0.17, respectively). Again, loading plots in form of S-plots were analyzed for the identification of the metabolites that were responsible for the clustering. In both cases, the Alt Maestrat samples showed high amounts of cycloartenol derivatives, whereas samples from the Mariola Mountains were rich in butyrospermol, lupeol, and *cis*-polyisoprene (Figure 5B). The Espadan samples had also high amounts of butyrospermol and were rich in lipidic esters. When samples from the Espadan and Mariola Mountains were compared, slighter differences were observed. Key metabolites responsible for the separation of these two groups of samples were *cis*-polyisoprene (in the Mariola Mountains) and 25-hydroperoxycycloart-23-en-3β-ol (in the Espadan Mountains).

Many variables can affect the metabolic profiling and thus cause differences between populations that grow wild in the three regions. For example, levels of plant metabolites can vary throughout the day, although these EC samples were harvested from each population at the same time of the day (in the morning) and throughout the same day/night rhythms (14 h light/10 h dark in July). Another important variable is the age of the plants, because different plant developmental stages can result in differences between metabolite profiles of young and old tissues. In this study, plant samples included both young and old tissues of mature plants of EC harvested after the flowering period (end of March−May), but all of them were harvested in the same way. Thus, in view of our results it seems that climatic and environmental factors may have greater influence than other variables in the metabolite profile of EC in summer. These results are coherent with the fact that plants in the Alt Maestrat grow in a different environment than plants in the Espadan and Mariola Mountains (in the higher and in the lower mesomediterranean bioclimatic belt, respectively). Therefore, there are many different important factors (precipitation, solar irradiance, temperature, humidity, and soil types) that may affect plant development and, consequently, the secondary metabolite biosynthesis and metabolite profile of these EC plants. For more detailed and precise conclusions, more samples taking into account all biological variations should be analyzed. However, with this preliminary result we have shown that this kind of analysis is appropriate for our platform.

MVA enabled a rapid classification of samples, and as has been shown in previous sections, ^{13}C spectroscopy also allows the

integration of specific regions for each metabolite permitting a targeted analysis of each compound. For comparative purposes, the mean integral values are presented together with the p values (Table 5). The least significant difference (LSD) between values obtained by the Tukey range test determined the existence of significant differences. Compounds were divided into four groups according to the p values obtained: (1) compounds that change only between stems and leaves, (2) compounds that change between regions, (3) compounds that change between stems and leaves and between regions, and (4) compounds that do not change systematically.

The integration values shown in Table 5 confirmed the results obtained from the MVA analysis. In leaves, there were larger quantities of alkanes, esters, and alcohols, whereas stems contained larger amounts of triterpenes. In particular, there were more lupen-3-one, butyrospermol, lanosterol, and cycloartenol derivatives in stems, whereas no important differences were found for α-amyrin, lupeol, and β-sitosterol. With regard to the different regions, once again the Alt Maestrat samples contained a different metabolite profile than the samples from the other two locations. As expected, they contained less butyrospermol and *cis*-polyisoprene, but also less α-amyrin and lupeol, whereas the concentrations of cycloartenol derivatives and β-sitosterol were higher.

On the other hand, if the goal of the study is a high-throughput and global analysis to provide sample classification but no exact quantification is required, an interesting option could be to acquire normal, nonquantitative ^{13}C spectra. This option could be similar to the widespread use of relaxation-edited NMR (CPMG), J-resolved, or diffusion-edited experiments in ^{1}H NMR metabolomics, none of them being quantitative.[39] To prove the validity of the conventional ^{13}C NMR and find differences between leaf and stem extracts similar to the previous study, we have acquired short (30 min), nonquantitative ^{13}C NMR spectra on a conventional probe of different EC extracts from the three regions. Again, a good separation between samples from stems and leaves was obtained with OPLS-DA (the corresponding score plot and S-plot can be found in the Supporting Information, Figure S-5), and very similar metabolites that were responsible for this separation could be identified. High levels of triterpenes and *cis*-polyisoprene were associated with stem samples, whereas high amounts of alkanes, esters, and free alcohols were found in leaf samples.

The present work has established a rapid and accurate method for the identification and quantification of the different nonpolar metabolites from complex plant extracts by quantitative ^{13}C NMR spectroscopy. The high chemical shift range of this technique together with the use of 2D experiments enabled an easy, unambiguous assignment that provided detailed information about the main primary and secondary metabolites of the three different plants. ^{13}C NMR allowed the quantification of different compound families as well as very specific and complex metabolites. The identification of a general integration region for triterpene derivatives offers a fast method to determine the triterpenes/paraffins ratio without the need of a further detailed assignment.

The data matrices obtained by this method proved to be suitable for the MVA and allowed the differentiation of the metabolite profile of plants grown in several regions and the possibility of detecting environmental influences on the metabolite biosynthesis. Important differences were also found between leaf and stem extracts. These results showed that ^{13}C NMR spectroscopy is suitable for metabolic profiling purposes.

■ ASSOCIATED CONTENT

Ⓢ Supporting Information. Tables S-1−S-3: ^{13}C spectral regions of metabolites used for integration. Figures S-1 and S-2: T_1 measurement experiments from *E. characias*. Figures S-3−S-5: OPLS-DA of EC samples from different regions. This material is available free of charge via the Internet at http://pubs.acs.org.

■ AUTHOR INFORMATION

Corresponding Author

*Phone: +34 963879058. Fax: +34 963879059. E-mail: ncabedo@ceqa.upv.es.

Funding Sources

We thank the Spanish Ministerio de Ciencia e Innovación of Spain (MICINN, SAF2008-01845) and the Centro de Investigación Príncipe Felipe for their economic support. We also thank Cemex Sustainable Chair in Spain for the predoctoral fellowship to P.V.E.

■ ACKNOWLEDGMENT

We acknowledge Antonio Fernández (Bruker) for technical NMR support.

■ REFERENCES

(1) Aliferis, K. A.; Tokousbalides, M. C. Metabolomics in pesticide research and development: review and future perspectives. *Metabolomics* **2011**, *7*, 35–53.

(2) Dixon, R. A.; Gang, D. R.; Charlton, A. J.; Fiehn, O.; Kuiper, H. A.; Reynolds, T. L.; Tjeerdema, R. S.; Jeffery, E. H.; German, J. B.; Ridley, W. P.; Seiber, J. N. Applications of metabolomics in agriculture. *J. Agric. Food Chem.* **2006**, *54*, 8984–8994.

(3) Colquhoun, I. J. Use of NMR for metabolic profiling in plant systems. *J. Pestic. Sci.* **2007**, *32*, 200–212.

(4) Riederer, M.; Schreiber, L. Protecting against water loss: analysis of the barrier properties of plant cuticles. *J. Exp. Bot.* **2001**, *52*, 2023–2032.

(5) Koops, A. J.; Baas, W. J.; Groeneveld, H. W. The composition of phytosterols, latex triterpenols and wax triterpenoids in the seedling of *Euphorbia lathyris* L. *Plant Sci.* **1991**, *74*, 185–191.

(6) Konno, K. Plant latex and other exudates as plant defense systems: roles of various defense chemicals and proteins contained therein. *Phytochemistry* **2011**, *72*, 1510–1530.

(7) Medina, E.; Aguilar, G.; Gómez, M.; Aranda, J.; Medina, J. D.; Winter, K. Taxonomic significance of the epicuticular wax composition in species of the genus *Clusia* from Panama. *Biochem. Syst. Ecol.* **2006**, *34*, 319–326.

(8) Kim, H. K.; Choi, Y. H.; Verpoorte, R. NMR-based metabolomic analysis of plants. *Nat. Protoc.* **2010**, *5*, 536–549.

(9) Choi, Y. H.; Sertic, S.; Kim, H. K.; Wilson, E. G.; Michopoulos, F.; Lefeber, A. W. M.; Erkelens, C.; Kricun, S. D. P.; Verpoorte, R. Classification of *Ilex* species based on metabolomic fingerprinting using nuclear magnetic resonance and multivariate data analysis. *J. Agric. Food. Chem.* **2005**, *53*, 1237–1245.

(10) Kovacs, H.; Moskau, D.; Spraul, M. Cryogenically cooled probes − a leap in NMR technology. *Prog. Nucl. Magn. Reson. Spectrosc.* **2005**, *46*, 131–155.

(11) Keun, H. C.; Beckonert, O.; Griffin, J. L.; Richter, C.; Moskau, D.; Lindon, J. C.; Nicholson, J. K. Cryogenic probe ^{13}C NMR spectroscopy of urine for metabonomic studies. *Anal. Chem.* **2002**, *74*, 4588–4593.

(12) Kubeczka, K. H.; Formácek, V. *Essential Oils Analysis by Capillary Gas Chromatography and Carbon 13 NMR Spectroscopy*, 2nd ed.; Wiley: New York, 2002.

(13) Vlahov, G.; Rinaldi, G.; Del Re, P.; Giuliani, A. A. ^{13}C nuclear magnetic resonance spectroscopy for determining the different components

of epicuticular waxes of olive fruit (*Olea europea*) Dritta cultivar. *Anal. Chim. Acta* **2008**, *624*, 184–194.

(14) Xia, Z.; Akim, L. G.; Argyropoulos, D. S. Quantitative ^{13}C NMR analysis of lignins with internal standards. *J. Agric. Food Chem.* **2001**, *49*, 3573–3578.

(15) Dunn, W. B.; Bailey, N. J. C.; Johnson, H. E. Measuring the metabolome: current analytical technologies. *Analyst* **2005**, *130*, 606–625.

(16) Sotak, C. H.; Dumoulin, C. L.; Levy, G. C. In *Topics in Carbon-13 NMR Spectroscopy*; Levy, G. C., Ed.; Wiley: New York, 1984; Vol 4, pp 91−121.

(17) Cabrera, G. M.; Seldes, A. M. Hydroperoxycycloartanes from *Tillandsia recurvata*. *J. Nat. Prod.* **1995**, *58*, 1920–1924.

(18) Bhattacharyya, J.; Barros, C. B. Triterpenoids of *Cnidosculus urens*. *Phytochemistry* **1986**, *25*, 274–276.

(19) Yoshida, K.; Hirose, Y.; Imai, Y.; Kondo, T. Conformational analysis of cycloartenol, 24-methylenecycloartenol and their derivatives. *Agric. Biol. Chem.* **1989**, *53*, 1901–1912.

(20) Wood, C. A.; Lee, K.; Vaisberg, A. J.; Kingston, D. G. I.; Neto, C. C.; Hammond, G. B. A bioactive spirolactone iridoid and triterpenoids from *Himatanthus sucuuba*. *Chem. Pharm. Bull.* **2001**, *49*, 1477–1478.

(21) Ross, A.; Schlotterbeck, G.; Dieterle, F.; Senn, H. NMR spectroscopy techniques for application to metabonomics. In *Handbook of Metabonomics and Metabolomics*; Lindon, J. C., Nicholson, J. K., Holmes, E., Eds.; Elsevier: Amsterdam, The Netherlands, 2007; pp 99−100.

(22) Wold, S.; Johansson, E.; Cocchi, M. PLS − partial least squares projections to latent structures. In *3D-QSAR in Drug Design: Theory, Methods and Applications*; Kubinyi, H., Ed.; Escom Science: Leiden, The Netherlands, 1993; pp 523−550.

(23) Jackson, J. E. *A User's Guide to Principal Components*; Wiley: New York, 1991.

(24) Bylesjö, M.; Rantalainen, M.; Cloarec, O.; Nicholson, J. K.; Holmes, E.; Trygg, J. OPLS discriminant analysis: combining the strengths of PLS-DA and SIMCA classification. *J. Chemom.* **2006**, *20*, 341–351.

(25) Bijlsma, S.; Bobeldijk, I.; Verheij, E. R.; Ramaker, R.; Kochhar, S.; Macdonald, I. A.; van Ommen, B.; Smilde, A. K. Large-scale human metabolomics studies: a strategy for data (pre-) processing and validation. *Anal. Chem.* **2006**, *78*, 567–574.

(26) Wiklund, S.; Johansson, E.; Sjöström, L.; Mellerowicz, E. J.; Edlund, U.; Shockcor, J. P.; Gottfries, J.; Mortiz, T.; Trygg, J. Visualization of GC/TOF-MS-based metabonomics data for identification of biochemically interesting compounds using OPLS class models. *Anal. Chem.* **2008**, *80*, 115–122.

(27) Wen, H.; Kang, S.; Song, Y.; Song, Y.; Sung, S. H.; Park, S. Differentation of cultivation sources of *Ganoderma lucidum* by NMR-based metabolomics approach. *Phytochem. Anal.* **2009**, *21*, 73–79.

(28) Lee, J. E.; Lee, B. J.; Chung, J. O.; Hwang, J. A.; Lee, S. L.; Lee, C. H.; Hong, Y. S. Geographical and climatic dependencies of green tea (*Camellia sinensis*) metabolites: a ^{1}H NMR-based metabolomics study. *J. Agric. Food Chem.* **2010**, *58*, 10582–10589.

(29) Evilia, R. F. Quantitative NMR spectroscopy. *Anal. Lett.* **2001**, *34*, 2227–2236.

(30) Adriaensens, P. J.; Karssenberg, F. G.; Gelan, J. M.; Mathot, V. B. F. Improved quantitative solution state ^{13}C NMR analysis of ethylene-1-octene copolymers. *Polymer* **2003**, *44*, 3483–3489.

(31) González-Coloma, A.; López-Balboa, C.; Santana, O.; Reina, M.; Fraga, B. M. Triterpene-based plant defenses. *Phytochem. Rev.* **2001**, *10*, 245–260.

(32) Hemmers, H.; Gülz, P. G.; Marner, F. J. Triterpenoids in epicuticular waxes of three European *Euphorbia* species. *Z. Naturforsch.* **1988**, *43C*, 799–805.

(33) Böszörményi, A.; Szarka, Sz.; Héthelyi, É.; Gyurján, I.; László, M.; Simándi, B.; Szóke, É.; Lemberkovics, É. Triterpenes in traditional and supercritical-fluid extracts of *Morus alba* leaf and stem bark. *Acta Chromatogr.* **2009**, *21*, 659–669.

(34) López de Medrano-Villar, M. J.; Bello, R.; Esplugues, J.; Primo-Yúfera, E.; Primo-Millo, J. Triterpenoid compounds from *Araujia sericifera* B. effects on the isolated uinea pig ileum. *Methods Find. Exp. Clin. Pharmacol.* **1997**, *19*, 515–520.

(35) Akihisa, T.; Yasukawa, K.; Yamaura, M.; Ukiya, M.; Kimura, Y.; Shimizu, N.; Arai, K. Triterpene alcohol and sterol ferulates from rice bran and their anti-inflamatory effetcs. *J. Agric. Food Chem.* **2000**, *48*, 2313–2319.

(36) Sousa, A. F.; Pinto, P. C. R. O.; Silvestre, A. J. D.; Neto, C. P. Triterpenic and other lipophilic components from industrial cork byproducts. *J. Agric. Food Chem.* **2006**, *54*, 6888–6893.

(37) Guinda, A.; Rada, M.; Delgado, T.; Gutiérrez-Adánez, P.; Castellano, J. M. Pentacyclic triterpenoids from olive fruit and leaf. *J. Agric. Food Chem.* **2010**, *58*, 9685–9691.

(38) Rivas Martínez, S. Bioclimatic belts of West Europe. Relations between bioclimate and plant ecosystems. In *Environment and Quality of Life: Climate and Global Change*; Duplessy, J. C., Pons, A., Fantechi, R., Eds.; Proc. Eur. School Clim. Nat. Hazards course, Arles, France; 1990; Commission of the European Communities: Luxembourg, 1991; pp 225−246.

(39) Beckonert, O.; Keun, H. C.; Ebbels, T. M. D.; Bundy, J.; Holmes, E.; Lindon, J. C.; Nicholson, J. K. Metabolic profiling, metabolomic and metabonomic procedures for NMR spectroscopy of urine, plasma, serum and tissue extracts. *Nat. Protoc.* **2007**, *2*, 2692–2703.